Polyprenol-phosphate-mannose-dependent mannosyltransferases are thought to be involved in these later reactions (11, 13), but only the fifth mannosyltransferase, PimE, has so far been identified (17). AcPIM4 has been thought to be the branching point from which LM/LAM biosynthesis diverges from the PIM biosynthetic pathway, and a lipoprotein, LpqW, is thought to be involved in controlling the metabolic flux at this branch point (18, 19). This branch point is structurally viable because the terminal two mannoses of AcPIM6 are α1,2-linked, whereas the LM/LAM mannan chain is α1,6-linked. LM is believed to be the precursor of LAM, but the precursor-product relationship has not been experimentally proven.

The linear α1,6-mannose chain of LM is synthesized by an α1,6-mannosyltransferase encoded by *MSMEG_4241* in *M. smegmatis* (8) or MptA in a related organism, *Corynebacterium glutamicum* (20). Deletion of *MSMEG_4241* results in the accumulation of an intermediate containing 5–20 mannose residues instead of mature LM containing 21–34 mannose residues (Fig. 1*A*). Accumulation of the LM_{5-20} intermediate suggests that there is another α1,6-mannosyltransferase that mediates the initial stage of LM synthesis up to LM_{5-20}. Another gene, *MSMEG_3111*, might potentially play a role in LM/LAM biosynthesis because it is homologous to an α1,6-mannosyltransferase of *Corynebacterium* LM (21). However, an *MSMEG_3111* gene deletion mutant showed no defects in LM/LAM production (21), leaving its precise function unclear.

MSMEG_4247 and its *M. tuberculosis* ortholog, Rv2181, are α1,2-mannosyltransferases involved in LM/LAM biosynthesis (22, 23). An *MSMEG_4247* gene deletion mutant produced LAM lacking the α1,2-monomannose side chains, suggesting that MSMEG_4247 is responsible for the addition of the α1,2-mannose branches onto the α1,6-mannose backbone of LAM. Interestingly, the *MSMEG_4247* gene deletion mutant failed to accumulate LM (22), suggesting an essential role for the α1,2-mannose branch in the accumulation of LM.

A number of mannosyltransferases involved in the PIM/LM/LAM biosynthetic pathway have now been identified, but it remains largely unknown how these enzymes coordinate and control the complex and overlapping pathways of PIM/LM/LAM synthesis. As part of our study of the *pimE* gene (17), we generated an *MSMEG_4247* gene deletion mutant. Here we report our analyses on the Δ*MSMEG_4247* mutant, revealing that controlling expression levels of MSMEG_4247 is critical for the proper synthesis of LM and LAM.

EXPERIMENTAL PROCEDURES

Mycobacterial Strains and Culture Conditions—Wild-type *M. smegmatis* strain mc^2155 (24) and derived mutants were grown at 30 °C in Middlebrook 7H9 broth (BD Biosciences) supplemented with 0.2% (w/v) glucose, 0.2% (v/v) glycerol, 15 mM NaCl, and 0.05% (v/v) Tween 80. Where appropriate, antibiotics at the following concentrations were used: 20 μg/ml streptomycin, 200 μg/ml hygromycin, or 20 μg/ml kanamycin. Samples were prepared at logarithmic growth phase (A_{600} nm = 0.5–1.0) unless otherwise indicated.

Gene Cloning and Complementation—A fragment containing the *MSMEG_4247* gene was PCR-amplified (primers 053/054; supplemental Table S1) from *M. smegmatis* genomic DNA and cloned into the MscI and EcoRI sites of the episomal expression vector, pHBJ334 (25), driven by a strong promoter of a mycobacterial heat shock protein hsp60 (Phsp60), resulting in pYAB143. To create an integrative vector, an XbaI/SpeI fragment of pYAB143, containing Phsp60, the *MSMEG_4247* gene, and the streptomycin resistance cassette, was blunt end-ligated with an SpeI/Eam1105I fragment of pMV361 (26), containing the attachment site and integrase gene, resulting in pYAB243. Site-directed mutagenesis was performed as described previously (17), using pYAB143 or pYAB250 as a template and primers 320/321, resulting in pYAB254 or pYAB255. Hygromycin-resistant versions of the expression vectors were constructed as follows: pYAB251 by replacing the streptomycin resistance cassette of pHBJ334, pYAB250 by replacing the streptomycin resistance cassette of pYAB143, and pYAB184 by replacing the kanamycin resistance cassette of pMV306 (26). For an expression vector driven by the endogenous promoter, the *MSMEG_4247* gene and 200 bp of upstream flanking sequence was PCR-amplified (primers 312/313) and ligated into the ClaI/XbaI sites of pYAB184, resulting in pYAB247. For the acetamide-inducible system, the *MSMEG_4241* gene was PCR-amplified (primers 329/330) and ligated into the BamHI/XbaI sites of pJAM2 (27), resulting in pYAB262. To make an acetamide-inducible MSMEG_4247 expression vector (pYAB246), the kanamycin resistance cassette of pJAM2 was first replaced by a streptomycin resistance cassette, resulting in pYAB040, and the HindIII/Bpu1102I fragment of pYAB143 containing the *MSMEG_4247* gene was blunt end-ligated into the BamHI site of pYAB040. These constructs were transfected into *M. smegmatis* wild-type strain mc^2155 and mutant cells by electroporation.

Lipid Extraction and Analysis—The cell wall lipids were extracted from the cell pellets as described previously (17). Extracted lipids were analyzed by high performance thin layer chromatography (HPTLC) using chloroform, methanol, 13 M ammonia, 1 M ammonium acetate, water (180:140:9:9:23, v/v/v/v/v) as a solvent. Orcinol or molybdenum blue staining was used to visualize PIMs or phospholipids, respectively.

LM and LAM Extraction and Analysis—After lipid extraction, the delipidated pellets were resuspended in five volumes of phenol saturated with Tris-EDTA buffer (pH 6.6) (Nacalai Tesque, Kyoto, Japan) and five volumes of water and extracted for 2 h at 55 °C. The extract was further purified by dialysis or octyl-Sepharose column chromatography (GE Healthcare) and electroelution (model 422 Electro-Eluter, Bio-Rad) from an SDS-polyacrylamide gel where appropriate. LM/LAM were separated by SDS-PAGE (10–20% gradient gel) and visualized using the ProQ Emerald 488 carbohydrate staining kit (Molecular Probes) and a fluoroimage analyzer (FLA-5000, Fujifilm).

*Metabolic Labeling of Δ*MSMEG_4247*—Cells were washed and resuspended in a fresh aliquot of Middlebrook 7H9 broth at 0.2 g/ml pellet. Cells were radiolabeled with 50 μCi/ml D-[2-^{3}H]mannose (20 Ci/mmol; American Radiolabeled Chemicals) for 15 min, washed in 7H9 broth to remove unincorporated radioactive mannose, and chased in 7H9 broth containing 1 mM

mannose. Extracted LM/LAM were separated by SDS-PAGE and visualized by fluorography.

Mannosidase Treatment—LM/LAM fractions, mixed with PIMs as internal controls, were treated with or without 0.4 milliunits of *Aspergillus saitoi* α1,2-mannosidase (Prozyme) for 24 h at 37 °C. The treatment was repeated three times. LM/LAM were repurified by phenol and analyzed by SDS-PAGE as described above. Intensity profiles were obtained by the Multi Gauge software (Fujifilm). PIMs were purified by 1-butanol/water (2:1, v/v) partitioning and analyzed by HPTLC.

High Performance Anion Exchange Chromatography (HPAEC)—Acetolysis was performed following a published protocol (28). Monosaccharides were released by 2 M trifluoroacetic acid at 100 °C for 2 h. Released carbohydrates were analyzed by a Nanospace high performance liquid chromatography system (Shiseido, Tokyo, Japan) equipped with Screbead II (2.0 × 250 mm) (Shiseido) as an anion exchange column, 50 mM sodium acetate in 0.1 M NaOH as a mobile phase, and a pulsed amperometric detector.

Western Blotting—Rabbit antibodies were raised against a mixture of two peptides from MSMEG_4241 (MTPTETHKPNPGLAEHVC and CRAPESAEATASRQ), MSMEG_4247 (RTHTGDAHETDEPLVPLC and MSKRQSPRGAGLAPC), or PimB′ (CEHLPPGVDTDRFAPDPD and CGARLAELLSGRREARQA) and affinity-purified. Cell lysates were prepared by bead beating as described previously (17). Proteins were fractionated by SDS-PAGE (10–20% gradient gel) under reducing conditions and blotted onto a polyvinylidene difluoride membrane (Millipore). The membrane was blocked with 5% skim milk and then incubated with a primary antibody (rabbit anti-MSMEG_4247, anti-MSMEG_4241, or anti-PimB′ antibodies; 1 μg/ml) for 1 h and a secondary antibody (anti-rabbit IgG antibody, horseradish peroxidase-conjugated; 1:2000 dilution; Amersham Biosciences) for 1 h. The bound probe was visualized by chemiluminescence (PerkinElmer Life Sciences). Images were captured by a luminescent image analyzer (LAS-4000, Fujifilm) and quantified by the Multi Gauge software.

Acetamide-induced Expression and Metabolic Labeling—Cells were grown in Middlebrook 7H9 medium, and 0.2% acetamide was added at midlog phase. After induction, the cells were washed in Sauton's medium (29), resuspended at 0.2 g/ml pellet, pulse-labeled with D-[2-^{3}H]mannose (24.7 Ci/mmol; PerkinElmer Life Sciences) for 15 min, and diluted 50-fold in Middlebrook 7H9 broth containing 1 mM mannose for chase. Extracted LM/LAM were separated by SDS-PAGE and visualized by fluorography.

Subcellular Fractionation—Cells were lysed by nitrogen cavitation, and the crude lysate was separated by a sucrose density gradient (25–56%) as described previously (30). Each fraction was tested for protein concentration, PIM biosynthetic activities (30), and Western blot detection of MSMEG_4247, MSMEG_4241, and PimB′.

RESULTS

Complementation of MSMEG_4247-deficient Mutant with MSMEG_4247 Does Not Restore the Synthesis of Normal LM and LAM—We deleted the *MSMEG_4247* gene by homologous recombination and confirmed the gene deletion by

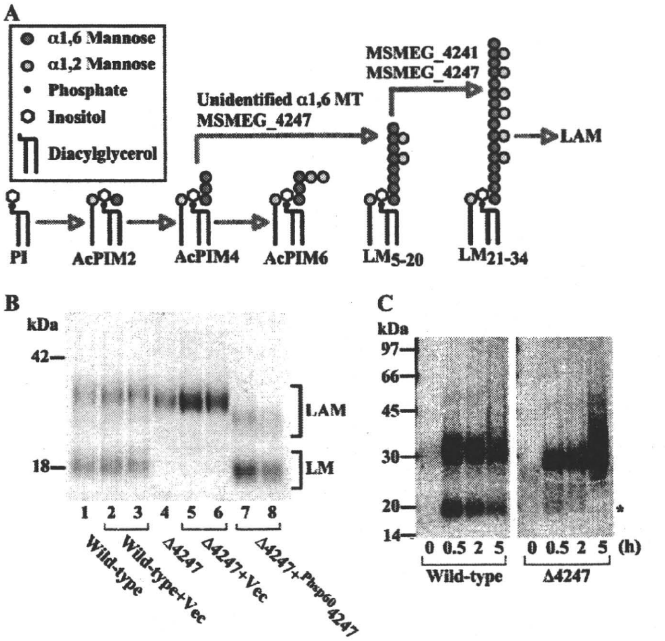

FIGURE 1. **The phenotype of *MSMEG_4247* deletion mutant (Δ*MSMEG_4247*) cannot be restored by introduction of the episomal MSMEG_4247 overexpression vector.** *A*, proposed pathway of PIM, LM, and LAM biosynthesis. Note that AcPIM4 is a proposed branch point from which the LM/LAM biosynthesis pathways diverge. The mannosyltransferase (*MT*) that mediates the initial elongation of the α1,6-mannose chain to produce LM_{5-20} has not been identified. The positions of the α1,2 side branches are hypothetical. Only the products and key intermediates are shown, and tetra-acylated PIMs are not shown for simplicity. *B*, LM/LAM from Δ*MSMEG_4247* and its complemented strains were analyzed by SDS-PAGE and visualized by carbohydrate staining. Wild-type (*lanes 1–3*) and Δ*MSMEG_4247* mutant (*lanes 4–8*) were transfected with an empty vector (*lanes 2, 3, 5,* and *6*, pYAB251) or an episomal ^{Phsp60}*MSMEG_4247* vector (*lanes 7* and *8*, pYAB250). Loading was adjusted for equal cell pellet equivalents. *C*, [^{3}H]mannose metabolic labeling of LM and LAM in the Δ*MSMEG_4247* mutant strain. Cells were pulsed with [^{3}H]mannose for 15 min and chased with excess non-radioactive mannose for up to 5 h. LM and LAM profiles were analyzed by SDS-PAGE and fluorography. Transient synthesis of LM is indicated by an *asterisk*.

Southern blotting (supplemental Fig. S1, *A* and *B*). We extracted LM and LAM from the deletion mutant and analyzed them by SDS-PAGE. We found even greater accumulation of LAM in the Δ*MSMEG_4247* mutant, but the mutant LAM appeared slightly smaller than that from wild type. More striking, the mutant lacked LM completely (Fig. 1*B*; wild type (*lanes 1–3*) and Δ*MSMEG_4247* (*lanes 4–6*)), as reported recently (see Fig. 2 of Ref. 22). The complete disappearance of LM was unexpected because the lack of the α1,2 side chain should still leave the α1,6 backbone intact. We considered the possibility that LM was synthesized but could not accumulate. To test this possibility, we radiolabeled the Δ*MSMEG_4247* mutant metabolically in a pulse-chase experiment using [^{3}H]mannose. The mutant cells produced a weakly radiolabeled species (Fig. 1*C*, *asterisk*), which had an electrophoretic mobility similar to that of wild-type LM. The radiolabeled LM in the wild-type cells remained during the 5-h chase period, whereas the mutant LM completely disappeared within 5 h, suggesting that LM could only accumulate transiently in the mutant. We next examined whether these phenotypes were rescued by the introduction of the MSMEG_4247 expression vector. We used an episomal expression vector, in which a strong hsp60

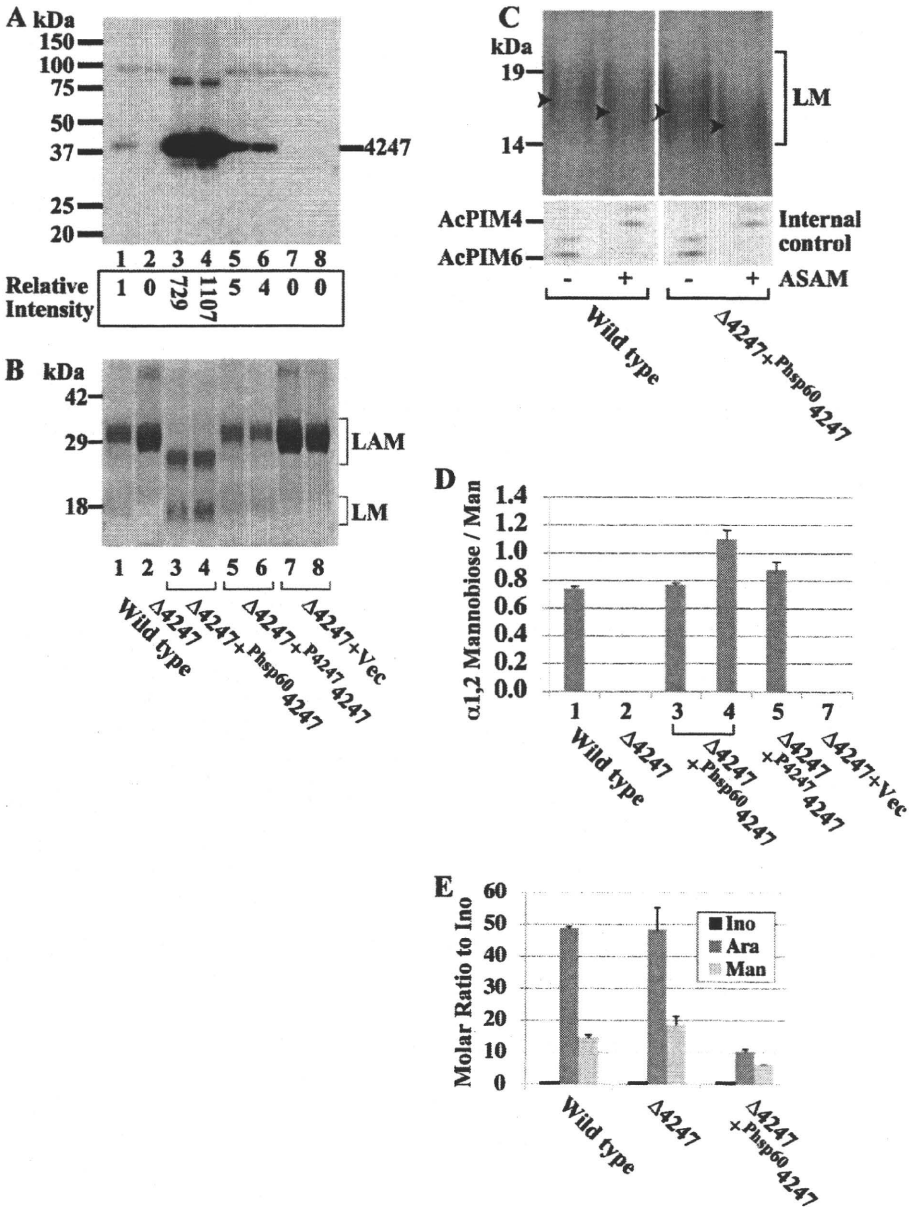

FIGURE 2. **Controlled expression of MSMEG_4247 is critical for the restoration of LM/LAM biosynthesis.** *A*, MSMEG_4247 expression examined by Western blotting using anti-MSMEG_4247 antibody. *Lane 1*, wild type; *lane 2*, Δ*MSMEG_4247*; *lanes 3* and *4*, two clones of Δ*MSMEG_4247*+^{Phsp60}*MSMEG_4247* (pYAB250); *lanes 5* and *6*, two clones of Δ*MSMEG_4247*+^{P4247}*MSMEG_4247* (pYAB247); *lanes 7* and *8*, two clones of Δ*MSMEG_4247* transfected with empty integrative vector (pYAB184). Loading was adjusted to 5 μg of protein/lane except for *lanes 3* and *4*, in which 1 μg of protein was loaded per lane. Relative intensities were calculated taking different protein loadings into account. *B*, LM/LAM profiles of *MSMEG_4247* deletion mutants complemented by various expression vectors. LM/LAM were analyzed by SDS-PAGE and visualized by carbohydrate staining. Lanes are arranged in the same order as in *A*. Faint doublet bands slightly above the 18 kDa marker seen in all *lanes* are protein contaminants. *C*, LM from wild-type or Δ*MSMEG_4247*+^{Phsp60}*MSMEG_4247* was treated with or without α1,2-mannosidase (*ASAM*), analyzed by SDS-PAGE using Tris-Tricine gel (15–20%) to improve the separation, and visualized by carbohydrate staining. Peak of LM in each *lane* was determined from the intensity profile and is indicated by an *arrowhead*. PIMs were included as internal controls and showed specific and complete digestion of the terminal two α1,2-mannoses of AcPIM6, producing AcPIM4. *D*, LM/LAM extracts were acetolyzed, and released mannose and α1,2-mannobiose were detected by HPAEC. Molar ratios of α1,2-mannobiose to mannose, measured in triplicate, are shown as averages with S.D. values. *Column numbers* specify the samples analyzed in the corresponding *lanes* in *A* and *B*. *E*, LAM was purified by electroelution and hydrolyzed by 2 M trifluoroacetic acid. Released carbohydrates were quantified by HPAEC. Data are presented as molar ratio relative to inositol. Averages of triplicate measurements with S.D. values are shown.

promoter (Phsp60) regulates the expression of MSMEG_4247 (26). Strikingly, the rescued mutant (Δ*MSMEG_4247*+^{Phsp60}*MSMEG_4247*) produced LM and LAM, but they were both smaller than those produced by the wild type (Fig. 1*B*, *lanes 7* and *8*).

Expression Level of MSMEG_4247 Is Critical for Controlling the Sizes of LM and LAM Produced—We considered the possibility that LM/LAM synthesis was prematurely terminated because of the high expression level of MSMEG_4247. We found that Δ*MSMEG_4247*+^{Phsp60}*MSMEG_4247* expressed MSMEG_4247 at >700 times the levels of the wild-type (Fig. 2*A*, compare *lanes 1* and *lanes 3* and *4*; note that the protein loading is 5 times less in *lanes 3* and *4*). To achieve a more controlled expression of MSMEG_4247, the Δ*MSMEG_4247* mutant was transfected with a vector carrying *MSMEG_4247* with its own upstream region instead of an artificial promoter. This vector lacks the mycobacterial origin of replication and instead carries the attachment site and the integrase gene from the mycobacteriophage L5, allowing for the site-specific integration of a single copy of the *MSMEG_4247* gene (26). Western blotting confirmed that the expression levels of MSMEG_4247 in the complemented strains (Δ*MSMEG_4247*+^{P4247}*MSMEG_4247*) were much closer to those of wild-type (4–5-fold overexpression; Fig. 2*A*, compare *lane 1* and *lanes 5* and *6*). As shown in Fig. 2*B*, LM and LAM from Δ*MSMEG_4247*+^{P4247}*MSMEG_4247* restored the migration pattern of wild-type LM and LAM (*lanes 5* and *6*). In contrast, Δ*MSMEG_4247*+^{Phsp60}*MSMEG_4247* reproducibly accumulated faster migrating LM and LAM (*lanes 3* and *4*). These results suggest that the sizes of LM and LAM are normalized if the Δ*MSMEG_4247* mutant is complemented with a wild-type level of MSMEG_4247 expression.

MSMEG_4247 is an α1,2-mannosyltransferase involved in the

transfer of the monomannose side chain. It was therefore perplexing that its overexpression resulted in smaller LM and LAM. To investigate whether the smaller sized LM and LAM produced in MSMEG_4247-overexpressing strains were modified by α1,2-mannose side chains, we removed the α1,2-mannose branches of LM by α1,2-specific mannosidase treatment and analyzed the size changes by SDS-PAGE (Fig. 2*C*). A shift of LM was detectable upon digestion of LM from both the wild-type and overexpressing strains. To confirm further, we acetolyzed the LM/LAM mixture from select strains and quantified the frequencies of α1,2-mannose branching. Acetolysis cleaves α1,6-mannose linkages without digesting α1,2-mannose linkages, producing α1,2-mannobiose and mannose. The ratio of α1,2-mannobiose to mannose indicates the ratio of mannoses with α1,2-mannose branches to those without. As shown in Fig. 2*D*, whereas the Δ*MSMEG_4247* mutant completely lacked the α1,2-mannose branch, LM/LAM from all complemented strains showed frequencies of α1,2-mannose branches comparable with those of the wild-type LM/LAM (*i.e.* ~45–50% of backbone mannoses were branched).

Despite the restoration of α1,2-mannose branching, LM and LAM from the Δ*MSMEG_4247*+^{Phsp60}*MSMEG_4247* strain appeared small on SDS-PAGE. To determine which component of LAM was responsible for the SDS-PAGE mobility shift, we purified LAM from an SDS-polyacrylamide gel by electroelution and analyzed its sugar composition. As shown in Fig. 2*E*, the Δ*MSMEG_4247* mutant did not show significant changes in the sugar compositions of LAM despite the lack of α1,2-mannose branches, suggesting that α1,6-mannose backbone is longer than that of wild-type LAM, and arabinosylation is occurring normally. The numbers of arabinose and mannose residues relative to inositol were somewhat smaller than previously reported (~70 arabinose and 21–34 mannose residues; see Introduction). This might be due to the contribution of inositol from inositol phosphate capping, a minor modification of LAM arabinan in *M. smegmatis* and other fast growing mycobacteria (31, 32). Strikingly, LAM from the Δ*MSMEG_4247*+^{Phsp60}*MSMEG_4247* strain showed greatly reduced numbers of arabinose and mannose. The mannan core carried less than half the number of mannose residues found in wild-type LAM. Because the frequency of the side-chain mannose is not significantly different between the dwarfed and wild-type LAM, these data suggest that the length of mannan backbone is less than half the length of wild-type LAM. Furthermore, arabinan was found to be 4 times smaller. This gross dwarfing is apparently the cause of faster migration on the SDS-polyacrylamide gel, although the protein molecular weight standards do not precisely reflect the actual molecular weight shifts of LM/LAM (see also Ref. 33 for another example). Taken together, our data suggested that overexpression of MSMEG_4247 restored the branches of α1,2-monomannose but prematurely terminated the elongation of the α1,6-mannose backbone and dwarfed the arabinan size.

Next we investigated whether the effect of MSMEG_4247 overexpression is specific to the LM/LAM pathway. Because LM/LAM biosynthetic pathways are thought to diverge from PIM biosynthesis at the AcPIM4 intermediate (see Fig. 1*A*), we examined the lipid fractions to see if there are any changes in the PIM or phospholipid profiles. We found no significant differences in either PIMs or phospholipids (supplemental Fig. S2), suggesting that the deletion or overexpression of MSMEG_4247 primarily affects LM/LAM biosynthesis.

Dwarfing LM/LAM Requires and Correlates with MSMEG_4247 Enzyme Activity—If the expression levels of MSMEG_4247 affect the elongation of the α1,6-mannose backbone, overexpression of MSMEG_4247 can affect the profile of LM and LAM in wild-type cells as well. To test this prediction, we introduced integrative or episomal MSMEG_4247 overexpression vectors and examined the effect of expression in the wild-type cells. Indeed, overexpression of MSMEG_4247 resulted in smaller LM and LAM in wild-type cells (Fig. 3*A*). A higher expression level was achieved using an episomal vector compared with an integrative vector. The hyperexpression in cells transfected with the episomal vector led to the production of LM and LAM, which appeared even smaller than the LM and LAM from cells transfected with the integrative vector (Fig. 3*A*, compare *lane 2* with *lanes 3* and *4*). To examine whether the production of smaller LM and LAM was dependent on the enzyme activity of MSMEG_4247, we created an MSMEG_4247 expression vector, in which the gene carried a site-directed mutation at a conserved aspartic acid residue. The aspartic acid residue 45 was conserved among mycobacterial species and aligned with the aspartic acid residue of PimE that is essential for enzymatic activity (supplemental Fig. S3*A*) (17). The expression of D45A-mutated MSMEG_4247 could not alter the LM/LAM profile of the Δ*MSMEG_4247* mutant, suggesting the loss of enzyme activity (supplemental Fig. S3, *B* and *C*). When introduced in the wild-type cells, the D45A mutant of MSMEG_4247 did not show a shift in the migration patterns of wild-type LM and LAM (Fig. 3*A*, *lanes 5* and *6*). The lack of effect was not due to the lack of expression of MSMEG_4247 D45A mutant because it was expressed at a level comparable with that of wild-type MSMEG_4247 (Fig. 3*B*, compare *lane 2* with *lanes 5* and *6*). These data further support our notion that the enzyme activity of MSMEG_4247 needs to be properly controlled to produce normal sized LM and LAM.

LM/LAM Biosynthesis Is Immediately Affected by Induced Expression of MSMEG_4247—Secondary mutations sometimes occur to compensate for an existing mutation in the genome, and secondary mutants with improved growth fitness can outgrow the original mutant. For example, deletion of the *lpqW* gene leads to spontaneous mutations in the *pimE* gene, resulting in an improved growth fitness of the mutant (18). We therefore wanted to exclude the possibility that the constitutive overexpression of MSMEG_4247 resulted in secondary mutations and that smaller LM/LAM was the consequence of these secondary mutations. To address this possibility, we created a vector, in which MSMEG_4247 expression was controlled by an acetamide-inducible promoter (27) and introduced this vector into wild-type cells. As shown in Fig. 4*A*, the acetamide-inducible promoter is leaky and expresses MSMEG_4247 at a level significantly higher than the wild-type level (compare *lanes 1* and *3*). Nevertheless, a much higher expression level was achieved after 4 h of acetamide induction (*lane 6*). At the 4-h time point, cells were metabolically pulse-

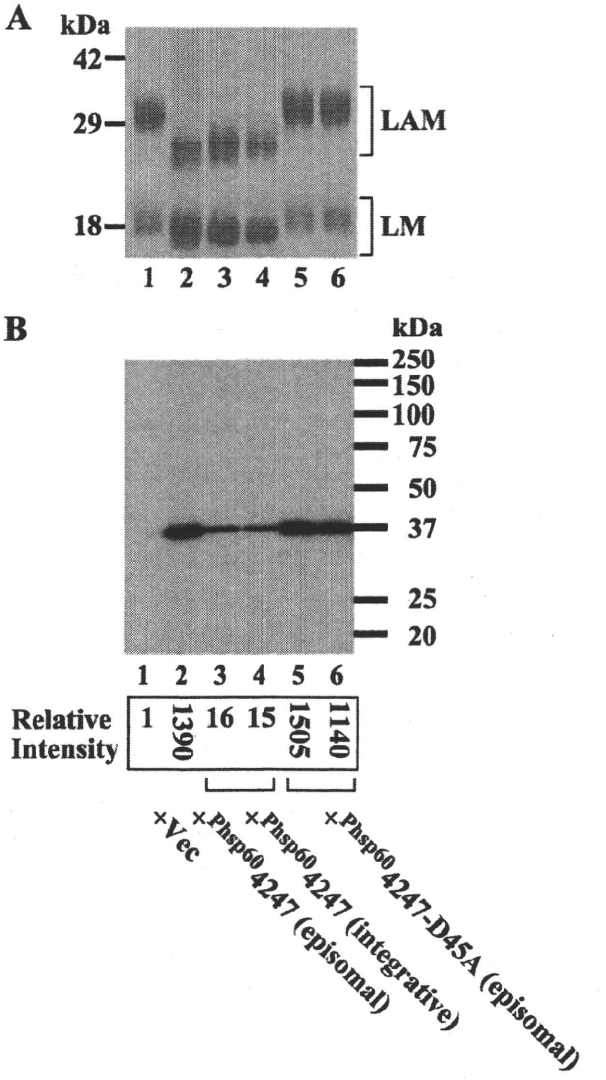

FIGURE 3. **Overexpression of MSMEG_4247 reduces the sizes of LM and LAM in wild-type cells.** *A*, LM/LAM profiles of wild-type cells transfected with various Phsp60-driven expression vectors were analyzed by SDS-PAGE and visualized by carbohydrate staining. *Lane 1*, empty vector (pHBJ334); *lane 2*, episomal vector to express MSMEG_4247 (pYAB143); *lanes 3* and *4*, integrative vector to express MSMEG_4247 (pYAB243); *lanes 5* and *6*, episomal vector to express MSMEG_4247 D45A mutant (pYAB254). *B*, MSMEG_4247 expression examined by Western blotting using anti-MSMEG_4247 antibody. *Lanes* are arranged in the same order as in *A*. Loading was adjusted to 5 μg of protein/lane for *lanes 1*, *3*, and *4* or 0.25 μg/lane for *lanes 2*, *5*, and *6*. Relative intensities were calculated, taking different protein loadings into account.

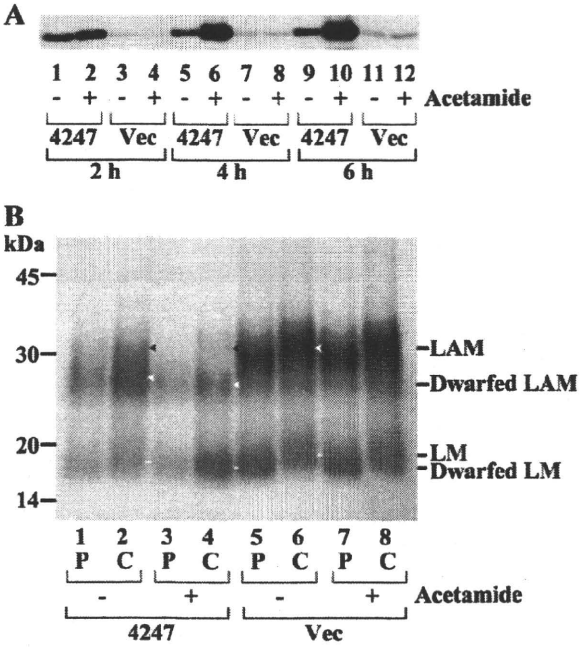

FIGURE 4. **Acetamide-induced overexpression of MSMEG_4247 prevents the maturation of LM/LAM.** *A*, acetamide induction of MSMEG_4247 examined by Western blotting using anti-MSMEG_4247 antibody. Wild-type cells transfected with either the acetamide-inducible MSMEG_4247 expression vector (*4247*) (transfected with pYAB246) or empty vector (*Vec*) (transfected with pYAB040) were incubated with (+) or without (−) acetamide for the indicated period to induce MSMEG_4247 expression. *B*, metabolic labeling with [^{3}H]mannose. Cells were incubated with (+) or without (−) acetamide for 4 h prior to radiolabeling. Cells were pulsed (*P*) for 15 min and then chased (*C*) in the presence of excess non-radioactive mannose for 25 min. The *white arrowheads* and *lines* indicate the peaks of LAM and LM, respectively, in *lanes 2*, *4*, and *6*, as determined by the intensity profiles shown in supplemental Fig. S4. The *black arrowheads* indicate the position of normal LAM as determined by the *white arrowhead* in *lane 6*.

labeled with [^{3}H]mannose and chased for 25 min in the presence of excess non-radioactive mannose (Fig. 4*B*). LM and LAM were relatively small in size immediately after pulse (*lanes* designated *P*). After the chase (*lanes* designated *C*), increased LM/LAM sizes were detected in control strains (compare *lanes 5* and *6* or *lanes 7* and *8*). Compared with control strains, the sizes of LM and LAM after chase remained smaller in the cells carrying acetamide-inducible MSMEG_4247 even without acetamide induction due to leaky expression of MSMEG_4247 (compare *lanes 2* and *6*; *white arrowheads* (LAM) and *white lines* (LM) indicate the peaks of the intensity profile shown in supplemental Fig. S4). Upon induction of MSMEG_4247 expression, production of normal sized LAM became even less efficient (compare *black arrowheads* in *lanes 2* and *4*), dwarfed LAM became even smaller (compare *white arrowheads* in *lanes 2* and *4*), and dwarfed LM became greater in intensity and slightly smaller in size (compare *white lines* in *lanes 2* and *4*). These observations suggest less efficient elongation of LM and LAM, being similar to those seen under constitutive overexpression of MSMEG_4247 (see Fig. 3*A*). Thus, MSMEG_4247 can exert its effect on LM/LAM biosynthesis immediately, and the timing appears to be too fast to be explained by secondary mutations.

The Effect of Overexpressed MSMEG_4247 Can Be Alleviated by the Overexpression of MSMEG_4241—Our data suggested that overexpressed MSMEG_4247 dominates the elongating enzymes, preventing the efficient elongation of the linear α1,6-mannose chain. We wanted to test if this effect of MSMEG_4247 overexpression can be competed by the overexpression of an elongating mannosyltransferase, MSMEG_4241. Therefore, we created another mutant in which an episomal vector for acetamide-inducible MSMEG_4241 expression was transfected into the MSMEG_4247 overexpressing strain (used in *lane 3* of Fig. 3). MSMEG_4241 expression was maximized at 4 h after the addition of acetamide (Fig. 5*A*). At this time point, we metabolically labeled cells with [^{3}H]mannose in a pulse-chase experiment. In control cells overexpressing MSMEG_4247 only, dwarfed LM immediately accumulated, and dwarfed

LAM also accumulated over time (Fig. 5*B*). When MSMEG_4241 overexpression was induced, we found little accumulation of dwarfed LM and identified a radiolabeled species migrating at around 35 kDa, which was comparable with wild-type LAM (Fig. 5*B*). The synthesis of normal size LM (~20 kDa) was less prominent, which might be due to the relative overexpression of MSMEG_4241. Next, we examined if the biosynthetic changes induced by the overexpression of MSMEG_4241 can lead into changes in cell wall composition of LM/LAM. Without acetamide induction, dwarfed LM and dwarfed LAM persisted over the 12-h time course (Fig. 5*C*, *left*). Being consistent with the metabolic labeling experiments, a species comparable with wild-type LAM started to appear at around 35 kDa after the 4-h induction and accumulated over the 12-h induction (Fig. 5*C*, *right*). In contrast to metabolic labeling, dwarfed LM persisted during the time course, suggesting a slow turnover rate of this species. We purified dwarfed LAM (from 0-h induction) and LAM-like species (from 12-h induction) by electroelution (Fig. 5*D*) and examined the sugar composition (Fig. 5*E*). The LAM-like species carried a mannan moiety with a size comparable with the wild-type LAM (see Fig. 2*E* for comparison). In contrast, arabinan size was only partially restored, suggesting that the rate of arabinan biosynthesis falls short of that of mannan biosynthesis when both elongating and branching mannosyltransferases are overexpressed in wild-type cells. These data together suggest that the dwarfing effect of overexpressed MSMEG_4247 can be partially overridden by MSMEG_4241 overexpression.

Spatial and Temporal Control of MSMEG_4241 and MSMEG_4247 Expressions in Wild-type Cells—The above results suggested that MSMEG_4247 and MSMEG_4241 function in close collaboration with each other during the synthesis of LM/LAM. Therefore, we predicted that these two enzymes are located

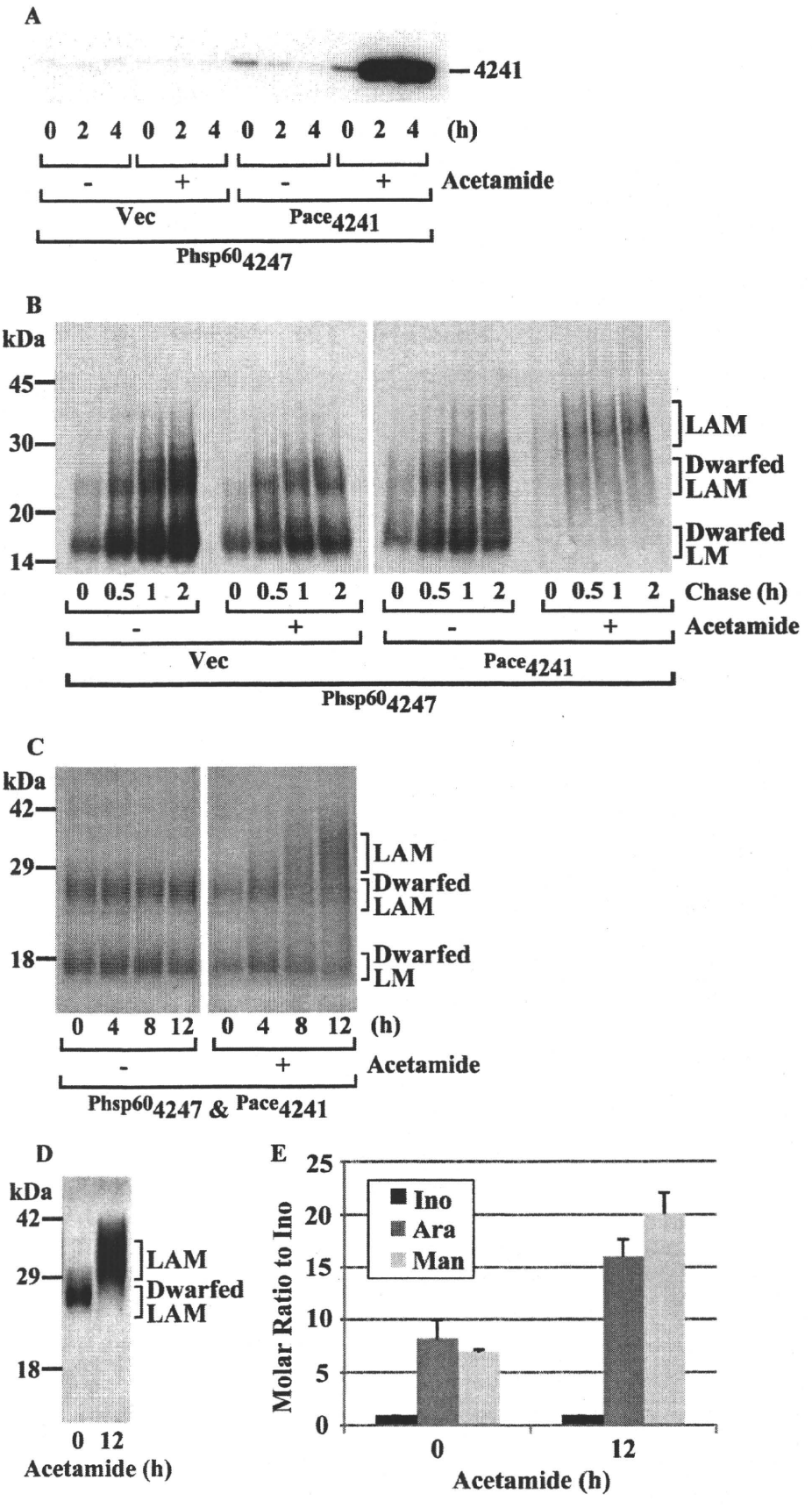

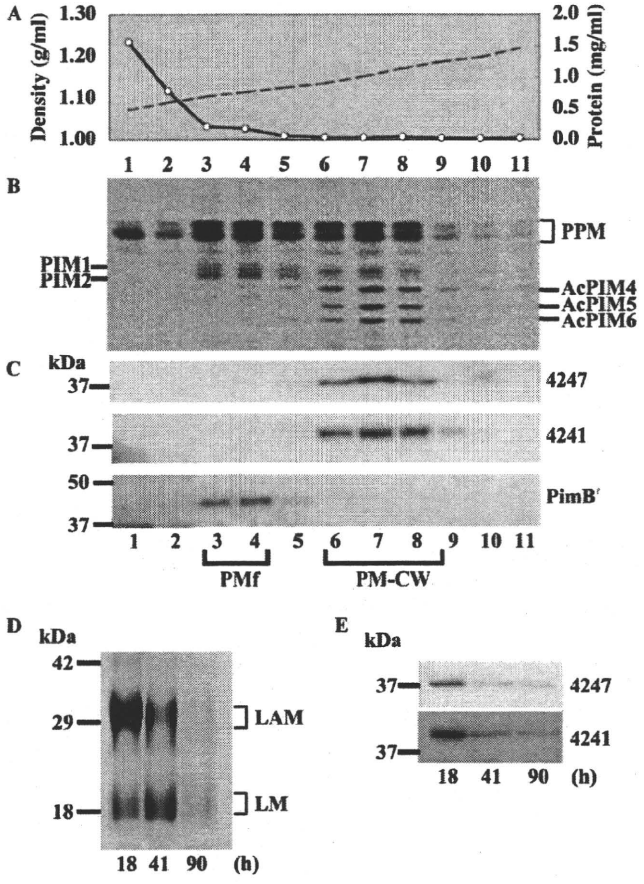

FIGURE 6. **Subcellular localization and growth phase-dependent expression of MSMEG_4247 and MSMEG_4241 in wild-type cells.** *A*, sucrose density (*dashed line*) and protein concentration (*open circle*) profiles of wild-type cell lysate fractionated by a density sedimentation. *B*, PIM biosynthetic activities of each fraction measured by GDP-[^{3}H]mannose radiolabeling. *PPM*, polyprenol-phosphate-mannose. *C*, Western blotting using anti-MSMEG_4247 (*top*), anti-MSMEG_4241 (*middle*), or anti-PimB' (*bottom*) antibodies. *D*, growth phase-dependent changes in LM/LAM levels of wild type cells grown in Middlebrook 7H9 broth. Culture was initiated by 1:100 dilution of a confluent starter culture, and aliquots were collected at the indicated time points, which correspond to logarithmic (18 h), early stationary (41 h), and late stationary (90 h) phases. Purified LM/LAM were separated by SDS-PAGE and visualized by carbohydrate staining. Loading was adjusted for equal cell pellet equivalents. *E*, growth phase-dependent changes in levels of MSMEG_4247 and MSMEG_4241 detected by Western blotting using anti-MSMEG_4247 or anti MSMEG_4241 antibodies. Loading was adjusted to 15 μg of protein/lane.

in the same domain of the plasma membrane. We tested this possibility using subcellular fractions of wild-type *M. smegmatis* (Fig. 6*A*). *M. smegmatis* has two functionally distinct membrane fractions designated PMf and PM-CW (30). PMf fractions contain membrane vesicles free of cell wall components, whereas PM-CW fractions represent plasma membranes tightly associated with the cell wall. PMf and PM-CW membranes can be separated by a sucrose density gradient sedimentation and are responsible for distinct biochemical reactions, such as the early (up to AcPIM2) and late (up to AcPIM6) parts of the PIM biosynthetic pathway, respectively (30) (Fig. 6*B*). As expected from the enriched PIM2 biosynthetic activities in PMf fractions (Fig. 6*B*), PimB' was specifically localized to these fractions (Fig. 6*C*). In contrast, MSMEG_4247 and MSMEG_4241 were both enriched in PM-CW fractions, suggesting that LM/LAM biosynthesis takes place in PM-CW fractions. These data are consistent with MSMEG_4247 and MSMEG_4241 acting in proximity to coordinate the LM/LAM biosynthesis. We have also tested co-immunoprecipitation of these two proteins to show their physical interaction, but it was not successful (data not shown; also see "Discussion"). Another interesting feature of LM/LAM biosynthesis is that it appears to be down-regulated in the late stationary phase (17) (Fig. 6*D*). Because imbalanced expressions of MSMEG_4247 and MSMEG_4241 can result in the production of aberrant forms of LM/LAM, we thought it important for the cells to down-regulate the expression levels of both enzymes in a concerted manner. Indeed, the expression levels of these two proteins were reduced simultaneously in the stationary phase (Fig. 6*E*), in correlation with the reducing levels of LM/LAM. Taken together, MSMEG_4247 and MSMEG_4241 were expressed in a temporally and spatially controlled manner.

Rv2181, an Ortholog of MSMEG_4247, Functions Similarly in M. tuberculosis—To examine whether the phenotypic characteristics of the Δ*MSMEG_4247* mutant were also displayed by other mycobacterial species, we generated an *M. tuberculosis* mutant in which the *Rv2181* gene, the *MSMEG_4247* ortholog, was deleted. The mutant was successfully generated (supplemental Fig. S5, *A* and *B*), and the Δ*Rv2181* mutant showed a smaller sized LAM and disappearance of LM (Fig. 7, *lane 2*), similar to the *M. smegmatis* mutant. When the *Rv2181* gene was introduced with its endogenous promoter region, LM synthesis was restored, and the size of LAM was also restored to that of wild-type LAM (*lanes 3* and *4*). When *Rv2181* was introduced via an integrative vector with Phsp60, the size of LM appeared normal, but the size of LAM appeared slightly smaller (*lanes 5* and *6*). Although the phenotypes are less prominent than those in *M. smegmatis*, these data highlight the conserved role of the α1,2-mannosyltransferase in producing properly sized LM and LAM.

DISCUSSION

Our analysis on MSMEG_4247, a branch-forming α1,2-mannosyltransferase involved in LM/LAM synthesis, revealed unexpected effects of its expression levels on the sizes and

FIGURE 5. **Dwarfing effect of MSMEG_4247 overexpression on LM/LAM can be competed by overexpression of MSMEG_4241.** *A*, acetamide induction of MSMEG_4241 examined by Western blotting using anti-MSMEG_4241 antibody. The MSMEG_4247 overexpression mutant was transfected with either acetamide-inducible MSMEG_4241 expression vector (*^{Pace}4241*) (transfected with pYAB262) or empty vector (*Vec*) (transfected with pJAM2) and incubated with (+) and without (−) acetamide for the indicated period to induce MSMEG_4241 expression. The loading was adjusted to 5 μg of protein/*lane*. *B*, metabolic labeling with [^{3}H]mannose. Cells were preincubated with (+) or without (−) acetamide for 4 h, pulsed for 15 min with [^{3}H]mannose, and then chased in the presence of excess non-radioactive mannose for up to 2 h. *C*, changes in total LM/LAM profiles after induction of MSMEG_4241 expression in MSMEG_4247 overexpression mutant. LM/LAM were separated by SDS-PAGE and visualized by carbohydrate staining. *D*, dwarfed LAM at 0 h and LAM-like species at 12 h after acetamide induction, shown in *C*, were purified by electroelution, and the purities were confirmed by SDS-PAGE and carbohydrate staining. *E*, compositional analysis of LAM-like species produced after MSMEG_4241 overexpression. Trifluoroacetic acid-hydrolyzed carbohydrates were quantified by HPAEC. Data are presented as molar ratio relative to inositol. Averages of triplicate measurements with S.D. values are shown.

quantities of LM/LAM (Fig. 8). Overexpression of MSMEG_4247 resulted in the production of dwarfed LM/LAM. In contrast, the deletion of MSMEG_4247 resulted in the disappearance of LM and accumulation of branchless LAM. We suggest that overexpression of the branching mannosyltransferase results in premature chain termination, whereas in the absence of branching, transiently synthesized branchless LM is either converted to LAM or degraded. Below, we discuss possible control mechanisms of mannan chain length and why branchless LM cannot be stably maintained.

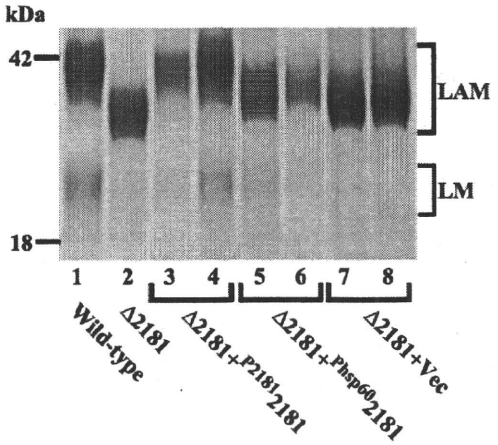

FIGURE 7. **LM/LAM profiles of *M. tuberculosis Rv2181* deletion mutants transfected with various expression vectors.** LM/LAM were extracted, analyzed by SDS-PAGE, and visualized by carbohydrate staining. *Lane 1*, wild type; *lane 2*, Δ*Rv2181* mutant; *lanes 3* and *4*, Δ*Rv2181* mutant transfected with pYAB228, an integrative expression vector carrying *Rv2181*, including 242 bp of upstream sequence; *lanes 5* and *6*, Δ*Rv2181* mutant transfected with pYAB230, an integrative expression vector carrying *Rv2181* driven by Phsp60; *lanes 7* and *8*, Δ*Rv2181* mutant transfected with pYAB184, an integrative empty vector control.

Most important, the following two pieces of evidence suggested that MSMEG_4247 affects the sizes of LM/LAM primarily by competing with the elongating α1,6-mannosyltransferase. First, we showed that 15-fold or more overexpression of MSMEG_4247 resulted in short α1,6-mannose backbone (see Figs. 2 and 3). Second, overexpression of elongating α1,6-mannosyltransferase (MSMEG_4241) alleviated the dwarfing effect of MSMEG_4247 overexpression (see Fig. 5). Dwarfed LM/LAM are unlikely to be caused by substrate depletion because MSMEG_4241 overexpression can at least partially override the dwarfing effect of MSMEG_4247 overexpression. It is tempting to speculate that MSMEG_4241 and MSMEG_4247 compete for the growing non-reducing terminus of mannan polymer, and MSMEG_4247-mediated α1,2-mannosylation of the non-reducing end blocks further elongation. Future studies using a cell-free assay system and synthetic substrates will address these possibilities.

Interestingly, overexpression of MSMEG_4247 resulted in the dwarfing of not only the mannan chain but the arabinan moiety of LAM (see Fig. 2*E*). Because both MSMEG_4241 and MSMEG_4247 are mannosyltransferases, it is unclear how the expression levels of these enzymes affect the arabinan size. One possibility is that multiple arabinans are attached to a single LAM molecule, and a short mannan chain limits the sites available for arabinosylation. In another experiment, we showed that overexpressed MSMEG_4241 competed with overexpressed MSMEG_4247 in terms of the LAM mannan size, but the restoration of the arabinan size was only partial (see Fig. 5). We speculate that relatively low (wild-type) expression levels of arabinosyltransferases compared with overexpressed mannosyltransferases have led to the reduction in arabinan size. Based on these observations, it is conceivable that the expression levels of arabinosyltransferases are also controlled in concert with the two mannosyltransferases to coordinate LAM synthesis in wild-type cells. Identification and characterization of the arabinosyltransferase that initiates the arabinan synthesis will provide further mechanistic insight into LAM biosynthesis.

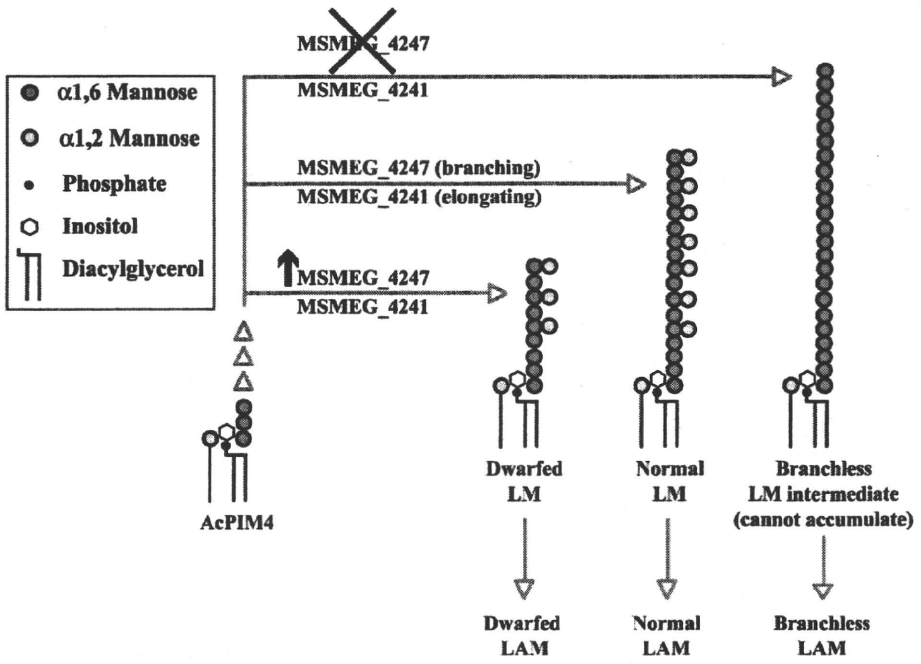

FIGURE 8. **A model of LM/LAM biosynthesis involving elongating (MSMEG_4241) and branching (MSMEG_4247) mannosyltransferases.** The lack of MSMEG_4247 results in the lack of LM and accumulation of branchless LAM. In contrast, overexpression of MSMEG_4247 results in dwarfed LM and dwarfed LAM. The positions of α1,2-mannose branches are hypothetical. Although our data are consistent with LM being a precursor of LAM biosynthesis, the precursor-product relationship of LM and LAM remains to be proved. The structure of LM intermediate in Δ*MSMEG_4247* mutant is hypothetical, based on the structure of LAM accumulating in the mutant.

The lack of α1,2-monomannose branching resulted in the complete absence of LM in both *M. smegmatis* and *M. tuberculosis* (see Figs. 1*B* and 7) (22), suggesting a conserved function of α1,2-mannose branching in LM accumulation. There are

several possibilities for why branchless LM cannot accumulate. First, in the absence of branching-dependent chain termination, MSMEG_4241 may be incapable of terminating the mannan polymerization by itself. We then speculate that arabinosylation acts as an alternative termination signal, thus resulting in the production of LAM only. Second, contrary to the first possibility, MSMEG_4241 may be able to terminate the polymer elongation after reaching a certain chain length, producing branchless LM. However, branchless LM cannot accumulate stably, perhaps because it is either efficiently converted to LAM or degraded. These possibilities are not exclusive to each other, and in either case, there appears to be an alternative chain termination mechanism in addition to mannose branching to control the mannan chain length. We consistently observed more enriched accumulation of branchless LAM in the *ΔMSMEG_4247* mutant compared with the wild-type levels. Although the precursor-product relationship of LM and LAM is not established, this observation favors the possibility that branchless LM intermediate is more avidly converted to LAM rather than being degraded. Curiously, although our *M. tuberculosis ΔRv2181* mutant showed a complete lack of LM, another recently reported *ΔRv2181* mutant accumulated small size LM (23). Further studies are necessary to identify factors that have led these two *ΔRv2181* mutants into different phenotypes.

At least a fraction of LAM synthesized in the plasma membrane appears to be transported to the surface layer of the cell wall (34), suggesting a dynamic spatial control of LAM biosynthesis. We demonstrated that both MSMEG_4247 and MSMEG_4241 are topologically confined in a membrane domain known as PM-CW (see Fig. 6, *A–C*), suggesting that LAM is synthesized in a spatially controlled manner, and these two enzymes may function in topological proximity. If MSMEG_4247 and MSMEG_4241 form a heterodimer, overexpression of kinetically inactive MSMEG_4247 may interfere with the formation of a functional dimer in the wild-type cells, leading to a phenotype similar to *ΔMSMEG_4247* mutant. However, such dominant negative effects were not observed (see Fig. 3*A*), making heterodimer formation less likely. We do not know if the levels of overexpression achieved in this study occur in physiological situations. Nevertheless, our results suggest that the expression levels of MSMEG_4247 and MSMEG_4241 need to be controlled in concert to avoid the production of aberrant LM/LAM. Being consistent with this suggestion, disappearance of LM/LAM in the stationary phase was closely correlated with concerted down-regulation of both enzymes (see Fig. 6, *D* and *E*). Interestingly, truncated structural variants of LAM have been identified in *Mycobacterium leprae* and clinical isolates of *M. tuberculosis* (33), implying that the polymer length of LM/LAM can vary among species/strains and may be controlled in response to environmental stimuli. Controlling the expression levels of MSMEG_4247 and MSMEG_4241 in *M. smegmatis* or their orthologs in other species may represent a key feature of the polymer length control of mycobacterial LM/LAM. Understanding the mechanisms of transcriptional and post-transcriptional controls of MSMEG_4247 and MSMEG_4241 expressions may provide further clues to understand the regulatory mechanisms of LM/LAM biosynthesis.

Acknowledgments—We thank Hidekazu Murakami, Dr. Morihisa Fujita, and Dr. Matthew Stokes for critical reading of the manuscript, Keiko Kinoshita for technical assistance, Dr. William R. Jacobs, Jr. (Albert Einstein College of Medicine) for kindly providing vectors pMV306 and pMV361, and Dr. Helen Billman-Jacobe (University of Melbourne) for kindly providing pJAM2 vector.

REFERENCES

1. Brennan, P. J. (2003) *Tuberculosis* **83,** 91–97
2. Briken, V., Porcelli, S. A., Besra, G. S., and Kremer, L. (2004) *Mol. Microbiol.* **53,** 391–403
3. Alderwick, L. J., Birch, H. L., Mishra, A. K., Eggeling, L., and Besra, G. S. (2007) *Biochem. Soc. Trans.* **35,** 1325–1328
4. Khoo, K. H., Dell, A., Morris, H. R., Brennan, P. J., and Chatterjee, D. (1995) *Glycobiology* **5,** 117–127
5. Lee, Y. C., and Ballou, C. E. (1964) *J. Biol. Chem.* **239,** 1316–1327
6. Brennan, P., and Ballou, C. E. (1967) *J. Biol. Chem.* **242,** 3046–3056
7. Khoo, K. H., Douglas, E., Azadi, P., Inamine, J. M., Besra, G. S., Mikusová, K., Brennan, P. J., and Chatterjee, D. (1996) *J. Biol. Chem.* **271,** 28682–28690
8. Kaur, D., McNeil, M. R., Khoo, K. H., Chatterjee, D., Crick, D. C., Jackson, M., and Brennan, P. J. (2007) *J. Biol. Chem.* **282,** 27133–27140
9. Chatterjee, D., Hunter, S. W., McNeil, M., and Brennan, P. J. (1992) *J. Biol. Chem.* **267,** 6228–6233
10. Shi, L., Berg, S., Lee, A., Spencer, J. S., Zhang, J., Vissa, V., McNeil, M. R., Khoo, K. H., and Chatterjee, D. (2006) *J. Biol. Chem.* **281,** 19512–19526
11. Besra, G. S., Morehouse, C. B., Rittner, C. M., Waechter, C. J., and Brennan, P. J. (1997) *J. Biol. Chem.* **272,** 18460–18466
12. Brennan, P., and Ballou, C. E. (1968) *J. Biol. Chem.* **243,** 2975–2984
13. Morita, Y. S., Patterson, J. H., Billman-Jacobe, H., and McConville, M. J. (2004) *Biochem. J.* **378,** 589–597
14. Guerin, M. E., Kaur, D., Somashekar, B. S., Gibbs, S., Gest, P., Chatterjee, D., Brennan, P. J., and Jackson, M. (2009) *J. Biol. Chem.* **284,** 25687–25696
15. Korduláková, J., Gilleron, M., Mikusova, K., Puzo, G., Brennan, P. J., Gicquel, B., and Jackson, M. (2002) *J. Biol. Chem.* **277,** 31335–31344
16. Korduláková, J., Gilleron, M., Puzo, G., Brennan, P. J., Gicquel, B., Mikusová, K., and Jackson, M. (2003) *J. Biol. Chem.* **278,** 36285–36295
17. Morita, Y. S., Sena, C. B., Waller, R. F., Kurokawa, K., Sernee, M. F., Nakatani, F., Haites, R. E., Billman-Jacobe, H., McConville, M. J., Maeda, Y., and Kinoshita, T. (2006) *J. Biol. Chem.* **281,** 25143–25155
18. Crellin, P. K., Kovacevic, S., Martin, K. L., Brammananth, R., Morita, Y. S., Billman-Jacobe, H., McConville, M. J., and Coppel, R. L. (2008) *J. Bacteriol.* **190,** 3690–3699
19. Kovacevic, S., Anderson, D., Morita, Y. S., Patterson, J., Haites, R., McMillan, B. N., Coppel, R., McConville, M. J., and Billman-Jacobe, H. (2006) *J. Biol. Chem.* **281,** 9011–9017
20. Mishra, A. K., Alderwick, L. J., Rittmann, D., Tatituri, R. V., Nigou, J., Gilleron, M., Eggeling, L., and Besra, G. S. (2007) *Mol. Microbiol.* **65,** 1503–1517
21. Mishra, A. K., Alderwick, L. J., Rittmann, D., Wang, C., Bhatt, A., Jacobs, W. R., Jr., Takayama, K., Eggeling, L., and Besra, G. S. (2008) *Mol. Microbiol.* **68,** 1595–1613
22. Kaur, D., Berg, S., Dinadayala, P., Gicquel, B., Chatterjee, D., McNeil, M. R., Vissa, V. D., Crick, D. C., Jackson, M., and Brennan, P. J. (2006) *Proc. Natl. Acad. Sci. U.S.A.* **103,** 13664–13669
23. Kaur, D., Obregón-Henao, A., Pham, H., Chatterjee, D., Brennan, P. J., and Jackson, M. (2008) *Proc. Natl. Acad. Sci. U.S.A.* **105,** 17973–17977
24. Snapper, S. B., Lugosi, L., Jekkel, A., Melton, R. E., Kieser, T., Bloom, B. R., and Jacobs, W. R., Jr. (1988) *Proc. Natl. Acad. Sci. U.S.A.* **85,** 6987–6991
25. Haites, R. E., Morita, Y. S., McConville, M. J., and Billman-Jacobe, H. (2005) *J. Biol. Chem.* **280,** 10981–10987
26. Stover, C. K., de la Cruz, V. F., Fuerst, T. R., Burlein, J. E., Benson, L. A., Bennett, L. T., Bansal, G. P., Young, J. F., Lee, M. H., and Hatfull, G. F. (1991) *Nature* **351,** 456–460
27. Triccas, J. A., Parish, T., Britton, W. J., and Gicquel, B. (1998) *FEMS Mi-*

crobiol. Lett. **167,** 151–156
28. Schneider, P., Ralton, J. E., McConville, M. J., and Ferguson, M. A. (1993) *Anal. Biochem.* **210,** 106–112
29. Sauton, B. (1912) *C. R. Acad. Sci. III* **155,** 860–863
30. Morita, Y. S., Velasquez, R., Taig, E., Waller, R. F., Patterson, J. H., Tull, D., Williams, S. J., Billman-Jacobe, H., and McConville, M. J. (2005) *J. Biol. Chem.* **280,** 21645–21652
31. Khoo, K. H., Dell, A., Morris, H. R., Brennan, P. J., and Chatterjee, D. (1995) *J. Biol. Chem.* **270,** 12380–12389
32. Gilleron, M., Himoudi, N., Adam, O., Constant, P., Venisse, A., Rivière, M., and Puzo, G. (1997) *J. Biol. Chem.* **272,** 117–124
33. Torrelles, J. B., Khoo, K. H., Sieling, P. A., Modlin, R. L., Zhang, N., Marques, A. M., Treumann, A., Rithner, C. D., Brennan, P. J., and Chatterjee, D. (2004) *J. Biol. Chem.* **279,** 41227–41239
34. Pitarque, S., Larrouy-Maumus, G., Payré, B., Jackson, M., Puzo, G., and Nigou, J. (2008) *Tuberculosis* **88,** 560–565